ELSEVIER

Journal of Organometallic Chemistry 637–639 (2001) 390–397

Journal of Organometallic Chemistry

www.elsevier.com/locate/jorganchem

Multistep redox properties of 2,2′-bipyridylboronium substituted ferrocenes

Li Ding [a], Kuangbiao Ma [a], Michael Bolte [b], Fabrizia Fabrizi de Biani [c], Piero Zanello [c], Matthias Wagner [a,*]

[a] *Institut für Anorganische Chemie, J.W. Goethe-Universität Frankfurt, Marie-Curie-Strasse 11, D-60439 Frankfurt (Main), Germany*
[b] *Institut für Organische Chemie, J.W. Goethe-Universität Frankfurt, Marie-Curie-Strasse 11, D-60439 Frankfurt (Main), Germany*
[c] *Dipartimento di Chimica dell'Università, Via Aldo Moro, I-53100 Siena, Italy*

Received 17 January 2001; received in revised form 23 April 2001; accepted 23 April 2001

Abstract

A high-yield synthesis and the X-ray crystal structure analysis of the dinuclear complex [FcB(bipy)OC_6H_4O(bipy)BFc]$(PF_6)_2$, **6**$(PF_6)_2$, which consists of two ferrocenyl moieties, two 2,2′-bipyridylboronium substituents and a hydroquinone linker, is described. The compound is perfectly stable toward air and moisture. **6**$(PF_6)_2$ exhibits a ferrocene-centered two-electron oxidation wave and two separate bipyridylboronium-centered two-electron reduction steps. No oxidation of the hydroquinone spacer takes place in the solvent window. **6**$(PF_6)_2$ is thus able to accept or deliver up to six electrons. Attempts to connect two [FcB(bipy)] fragments using glycol rather than hydroquinone as the bridging element gave the mononuclear complex [FcB(bipy)$O(CH_2)_2OH]PF_6$ only. A similar reaction scheme that was applied for the generation of [FcB(bipy)$O(CH_2)_2OH]PF_6$ was employed to synthesize the diol {1,1′-[$HO(CH_2)_2$OB(bipy)]2fc}$(PF_6)_2$; fc = $[(C_5H_4)_2Fe]$. This compound is able to store up to five electrons and may find use as a monomer for the generation of cationic, redox-active polyesters and polyurethanes. © 2001 Elsevier Science B.V. All rights reserved.

Keywords: Ferrocene; 2,2′-Bipyridylboronium cations; Oligonuclear complexes; Cyclic voltammetry; X-ray crystal structure analysis

1. Introduction

Transition metal-based polymers are of considerable current interest due to the fact that numerous specimens belonging to this class of compounds possess promising electronic and magnetic properties or show pronounced non-linear optical effects [1–7]. Among all the versatile building blocks used today, metallocenes exhibit particularly intriguing features, and much effort has been focused on the synthesis of poly(metallocene)s. Although the discovery of ring-opening polymerization (ROP) led to a breakthrough in poly(metallocene) synthesis [2], the development of this area still offers considerable synthetic difficulties.

We have recently reported on the facile synthesis of ferrocene derivatives bearing up to four 2,2′-bipyridylboronium substituents (**A1**–**A3**, Fig. 1) [8].

Similar to the related electron acceptor Diquat (Fig. 1), the 2,2′-bipyridylboronium moieties behave as reversible two-step redox systems in DMF solution [9].

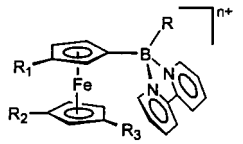

R = Me, Br, OMe; NMe_2
A1: R_1,R_2,R_3=H, n=1
A2: R_1,R_3=H, R_2=B(R)bipy, n=2
A3: R_1,R_2,R_3=B(R)bipy, n=4

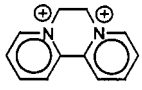

Diquat

Fig. 1. Highly redox-active ferrocene derivatives bearing 2,2′-bipyridylboronium substituents.

* Corresponding author. Fax: +49-69-798-29260.
E-mail address: matthias.wagner@chemie.uni-frankfurt.de (M. Wagner).

0022-328X/01/$ - see front matter © 2001 Elsevier Science B.V. All rights reserved.
PII: S0022-328X(01)00942-1

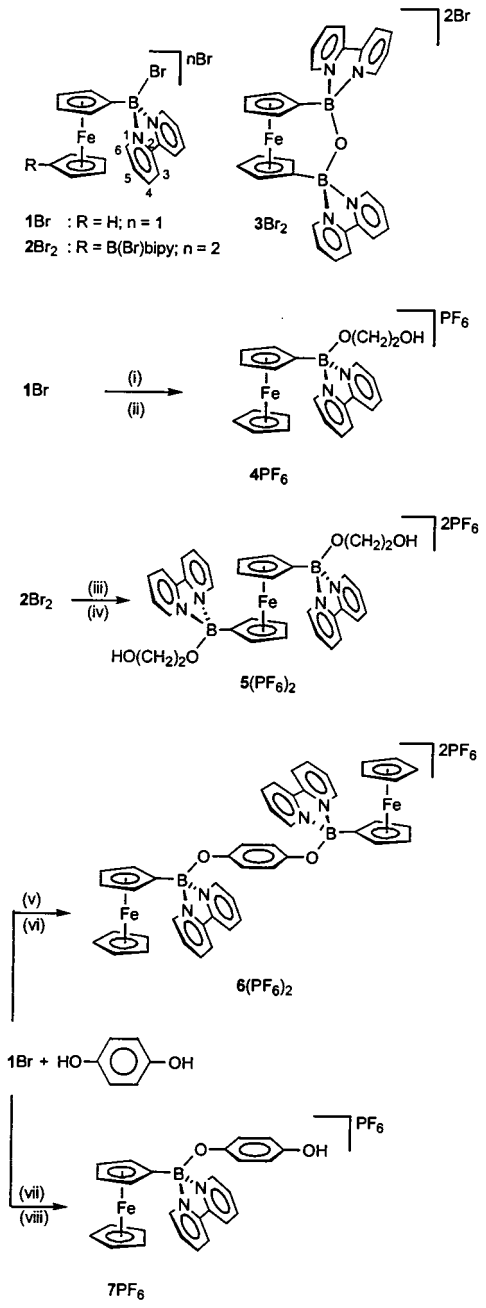

Scheme 1. (i) + exc. glycol, r.t.; (ii) + exc. NH_4PF_6, H_2O, r.t. (iii) + exc. glycol, r.t.; (iv) + exc. NH_4PF_6, H_2O, r.t. (v) + 0.5 equivalent hydroquinone, + one equivalent NEt_3, − 40 °C; (vi) + exc. NH_4PF_6, H_2O, r.t. (vii) + one equivalent hydroquinone/NEt_3, r.t. (viii) + exc. NH_4PF_6, H_2O, r.t.

Compounds **A**, which are highly soluble in polar solvents (e.g. DMF, DMSO, acetonitrile), can thus accept or deliver three (**A1**) to nine (**A3**) electrons [8]. Consequently, oligomeric aggregates of these redox-active compounds might be useful in the development of novel electron storage media.

Oligomerization of **A** might be achieved, for example, by linking the individual monomers via their boron atoms. Bromo substituents R at the boron centers of **A** are substituted easily by various nucleophiles (e.g. amines, alcohols) [8]. Difunctional nucleophiles can thus be expected to act as efficient bridging elements in the synthesis of larger aggregates of **A**.

This paper focuses on the reactions of mono- (**1**Br) and diborylated (**2**Br_2) ferrocenes with glycol and hydroquinone (Scheme 1).

The resulting complexes will supply valuable information about the electrochemical behavior of the material. Moreover, they will help to evaluate the perspective of our approach regarding polymer synthesis.

2. Results and discussion

2.1. Syntheses

The shortest possible bridge between two borylated ferrocene units would be a boron–boron bond or a single atom between the two boron centers. However, up to now, attempts to connect diborylated ferrocenes **2**Br_2 via B–O–B linkers by controlled hydrolysis of their B–Br bonds always led to the *ansa*-bridged complex **3**Br_2 as the result of an *intra*- rather than an *inter*-molecular reaction [10]. No polymeric material could be isolated, irrespective of the experimental conditions applied. The reaction of **2**Br_2 with aniline in the presence of triethylamine, on the other hand, was much slower and stopped at the monoborylamine stage without formation of diborylamine linkers [11]. For our purposes, O-nucleophiles thus appear to be superior over N-nucleophiles, however, the size of the bridging unit has to be increased in order to disfavor *ansa*-ferrocene formation.

On the basis of these considerations, two equivalents of **1**Br were treated with one equivalent of glycol and triethylamine in CH_2Cl_2. The reaction, which proceeded reluctantly and was accompanied by the formation of undesired side products (e.g. C–B bond cleavage), gave the 1:1 complex **4**PF_6 as a major component of the resulting mixture. The aimed-for dinuclear aggregates were not formed. To prove the chemical composition of **4**PF_6, the bromo derivative **1**Br was dissolved in neat glycol in the presence of triethylamine. The resulting mixture was added dropwise to an aqueous solution of NH_4PF_6. By this method, an analytically pure sample of the air and moisture stable compound **4**PF_6 was obtained in good yield. In an analogous way, **5**$(PF_6)_2$ can be synthesized from glycol and **2**Br_2.

As a consequence of the results obtained with the aliphatic diol, the aryl alcohol hydroquinone was chosen as an alternative bridge to generate the desired ferrocene-containing aggregates. Reaction of **1**Br with hydroquinone in a molar ratio of 2:1 led to the air- and moisture-stable dinuclear complex **6**Br_2. The corre-

sponding salt **6**$(PF_6)_2$ is moderately soluble in polar solvents like DMSO and acetonitrile. Aiming at the next higher trimeric complex, we have first isolated **7**PF_6 from **1**Br and hydroquinone (Scheme 1) and then treated two equivalents of **7**PF_6/triethylamine with one equivalent of **2**Br_2 in acetonitrile. The resulting material was insoluble in all common solvents and thus not characterized any further.

2.2. NMR spectroscopy

The ^{11}B-NMR signals of all products reported here lie in the range from -3.7 to 12.3 ppm, which is typical of tetracoordinate boron nuclei [12]. The ^{1}H- and ^{13}C-NMR spectra of **4**PF_6, **5**$(PF_6)_2$, **6**$(PF_6)_2$ and **7**Br exhibit the same general features for the ferrocene and [B(R)bipy] fragments (bipy: 2,2′-bipyridine): similar to the starting materials **1**Br and **2**Br_2 [8], the ferrocene moieties give rise to only one set of signals. The same is true for the bipy ligands. This finding points towards an unhindered rotation about the B–C and the B–O axes in the respective compounds. All chemical shifts lie in the usually observed ranges (e.g. the proton signals of the chelating bipy ligands appear at lower field compared to free 2,2′-bipyridine). In the ^{1}H-NMR spectrum, the dinuclear complex **6**$(PF_6)_2$ and the monomeric compound **7**Br exhibit characteristic differences. The hydroquinone bridge of the former gives rise to only one resonance [$\delta(^1H) = 6.03$] due to the high symmetry of the molecular framework, while the 1,4-phenylene spacer of the latter shows two signals [$\delta(^1H) = 6.34$ and 6.26] because of its less symmetric environment. An analogous pattern is observed in the ^{13}C-NMR spectra of both compounds.

2.3. Molecular structures of *4*PF_6, *6*$(PF_6)_2$ and *7*PF_6 in the solid state

X-ray-quality crystals of **4**PF_6 (orthorhombic; $Pna2_1$), **6**$(PF_6)_2$ (monoclinic; $P2_1/c$) and **7**PF_6 (monoclinic; $P2_1/c$) were grown by gas phase diffusion of diethyl ether into their acetonitrile solutions (Tables 1 and 2; Figs. 2–4).

As has already been deduced from the NMR spectra, tetracoordinate boron atoms are present in all the molecular structures. The dinuclear compound **6**$(PF_6)_2$

Table 1
Crystal data and structure refinement details of **4**PF_6, **6**$(PF_6)_2$ and **7**PF_6

	4PF_6	**6**$(PF_6)_2$	**7**PF_6
Empirical formula	$C_{22}H_{22}BF_6FeN_2O_2P$	$C_{46}H_{38}B_2F_{12}Fe_2N_4O_2P_2 \times 2\ C_2H_3N$	$C_{26}H_{22}BF_6FeN_2O_2P \times 0.5C_4H_{10}O$
Formula weight (g mol^{-1})	558.05	1184.17	643.15
Temperature (K)	173	173	173
Crystal system	Orthorhombic	Monoclinic	Monoclinic
Space group	$Pna2_1$	$P2_1/c$	$P2_1/c$
Unit cell dimensions			
a (Å)	18.172(1)	8.8453(9)	11.393(2)
b (Å)	14.506(1)	19.484(2)	16.545(2)
c (Å)	8.558(1)	14.549(1)	14.961(2)
α (°)	90	90	90
β (°)	90	102.811(4)	91.64(1)
γ (°)	90	90	90
V (Å^3)	2255.9(3)	2445.0(4)	2819.0(7)
Z	4	2	4
D_{calc} (g cm^{-3})	1.643	1.608	1.515
Crystal size (mm)	$0.65 \times 0.25 \times 0.05$	$0.52 \times 0.12 \times 0.08$	$0.50 \times 0.10 \times 0.10$
Radiation (Mo–K_α) (Å)	0.71073	0.71073	0.71073
Number of total reflections	27502	47187	16924
Number of unique reflections	4461	6310	5324
R_{int}	0.055	0.097	0.077
Number of parameters	320	344	376
μ (cm^{-1})	8.13	7.54	6.63
Final R_1 [a] [$I > 2\sigma(I)$]	0.0418	0.0601	0.0526
Final R_1 [a] (all data)	0.0530	0.1484	0.1002
Final wR_2 [b] [$I > 2\sigma(I)$]	0.0937	0.0905	0.1094
Final wR_2 [b] (all data)	0.0997	0.1134	0.1272
Goodness-of-fit on F^2 [c]	1.067	1.015	1.025

[a] $R_1 = \Sigma(\|F_o| - |F_c\|)/\Sigma|F_o|$.
[b] $wR_2 = [\Sigma w(F_o^2 - F_c^2)^2/\Sigma w(F_o^2)^2$.
[c] Goodness-of-fit $= [\Sigma w(F_o^2 - F_c^2)^2/(NO - NV)]^{1/2}$.

Table 2
Selected bond lengths (Å), bond angles (°) and torsion angles (°) of $\mathbf{4}PF_6$, $\mathbf{6}(PF_6)_2$ and $\mathbf{7}PF_6$

	$\mathbf{4}PF_6$	$\mathbf{6}(PF_6)_2$	$\mathbf{7}PF_6$
B(1)–O(1)	1.397(5)	1.434(4)	1.431(5)
B(1)–C(11)	1.570(5)	1.581(5)	1.573(6)
B(1)–N(21)	1.631(5)	1.599(4)	1.613(5)
B(1)–N(31)	1.628(5)	1.609(4)	1.631(5)
N(21)–C(22)	1.352(5)	1.355(4)	1.354(4)
N(31)–C(32)	1.354(5)	1.358(4)	1.347(4)
C(22)–C(32)	1.471(5)	1.460(4)	1.463(5)
N(21)–B(1)–N(31)	92.9(3)	94.7(2)	93.4(3)
N(21)–B(1)–O(1)	113.0(3)	108.5(3)	112.5(3)
N(31)–B(1)–O(1)	113.4(3)	108.6(3)	110.0(3)
N(21)–B(1)–C(11)	108.0(3)	112.4(3)	113.6(3)
N(31)–B(1)–C(11)	111.8(3)	112.4(3)	111.3(3)
O(1)–B(1)–C(11)	115.4(3)	117.7(3)	114.2(3)
B(1)–N(21)–C(22)	113.9(3)	113.3(3)	113.6(3)
B(1)–N(31)–C(32)	113.9(3)	112.6(3)	113.8(3)
N(21)–C(22)–C(32)	109.1(3)	109.1(3)	109.8(3)
N(31)–C(32)–C(22)	109.3(3)	109.6(3)	109.0(3)
C(23)–C(22)–C(32)	128.7(4)	129.5(3)	128.3(3)
C(33)–C(32)–C(22)	128.9(4)	129.2(3)	129.2(3)
O(1)–B(1)–C(11)–C(12)	148.3(4)	−99.9(4)	40.3(5)
N(21)–C(22)–C(32)–N(31)	−3.4(4)	2.3(3)	0.3(4)
C(23)–C(22)–C(32)–C(33)	−4.7(6)	2.5(5)	0.9(7)

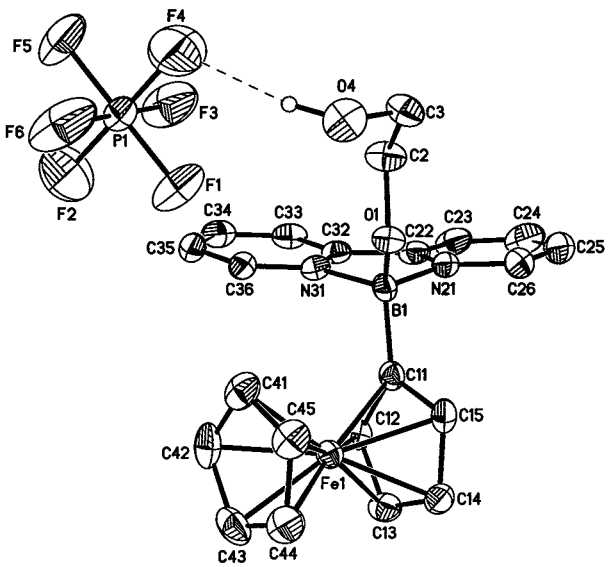

Fig. 2. Plot of $\mathbf{4}PF_6$; thermal ellipsoids are drawn at the 50% probability level.

possesses somewhat shorter B–N bond lengths [B–N(21) 1.599(4) Å; B–N(31) 1.609(4) Å] than the monomeric complexes $\mathbf{4}PF_6$ [B–N(21) 1.631(5) Å; B–N(31) 1.628(5) Å] and $\mathbf{7}PF_6$ [B–N(21) 1.613(5) Å; B–N(31) 1.631(5) Å]. The B(1)–O(1) bonds in the hydroquinone-containing species $[\mathbf{6}(PF_6)_2$: 1.434(4) Å; $\mathbf{7}PF_6$:1.431(5) Å] are longer than the boron–oxygen bond in the glycol derivative $\mathbf{4}PF_6$ [1.397(5) Å]. The 2,2′-bipyridylboronium fragments exhibit almost planar conformations with torsion angles between both pyridyl rings ranging from 0.3(4) to 3.4(4)°. Coordination of the small boron centers results in a distortion of the chelating bipy ligands. In the case of $\mathbf{6}(PF_6)_2$, for example, the angles C(23)–C(22)–C(32) and C(33)–C(32)–C(22) on the outer frame of the aromatic system are stretched to values of 129.5(3) and 129.2(3)°, respectively. Consequently, the angles N(21)–C(22)–C(32) and N(31)–C(32)–C(22) on the inside of the five-membered heterocycle are compressed to values of 109.1(3) and 109.6(3)°, respectively. The B(OR)bipy substituents in $\mathbf{4}PF_6$ and $\mathbf{7}PF_6$ are turned away from the central iron atom with torsion angles O(1)–B(1)–C(11)–C(12) of

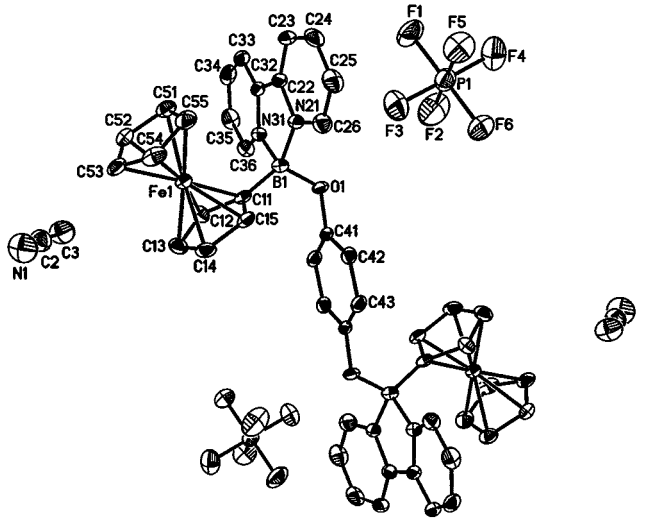

Fig. 3. Plot of $\mathbf{6}(PF_6)_2$; thermal ellipsoids are drawn at the 50% probability level.

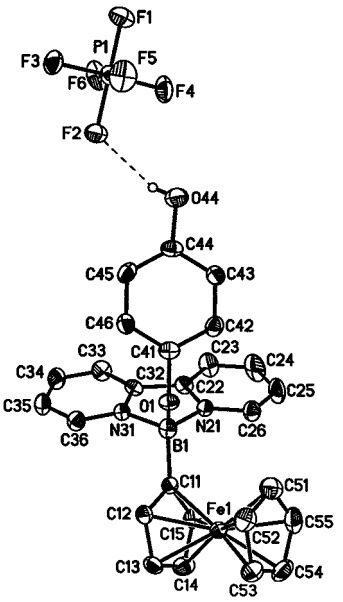

Fig. 4. Plot of $\mathbf{7}PF_6$; thermal ellipsoids are drawn at the 50% probability level. Ether molecule omitted for clarity.

Table 3
Formal electrode potentials (V, vs. SCE) and peak-to-peak separations (mV) for the redox changes exhibited by **4**PF_6, **6**$(PF_6)_2$ and **7**PF_6

Complex	Oxidation processes			Reduction processes			Solvent
	E_p [a]	$E°'$	ΔE_p [b]	$E°'$	ΔE_p [b]	$E°'$	ΔE_p [b]	
4PF_6	–	+0.45	60	−0.85	72	−1.48	68	DMF [c]
	–	+0.44	63	−0.84	63	−1.66 [a,b]	–	CH_2Cl_2 [d]
7PF_6	+1.34 [b]	+0.41	60	−0.86	50	−1.73 [a,b]	–	CH_2Cl_2 [d]
6$(PF_6)_2$	–	+0.50 [e]	66	−0.78	99	−1.48 [a,b,f]	–	DMF [c]
	–	+0.44 [e]	61	−0.86	45	−1.60 [a,b,f]	–	CH_2Cl_2 [d]
A1 [g]	–	+0.40	64	−1.02	64	−1.71	66	DMF [c]
	–	+0.42	66	−0.99	70	−1.79 [a]	–	CH_2Cl_2 [d]
FcH	–	+0.49	60	–	–	–	–	DMF [c]
	–	+0.39	78	–	–	–	–	CH_2Cl_2 [d]

[a] Peak-potential value for irreversible process.
[b] Measured at 0.1 V s^{-1}.
[c] $[NEt_4]PF_6$ (0.1 mol dm^{-3}) supporting electrolyte.
[d] $[NBu_4]PF_6$ (0.2 mol dm^{-3}) supporting electrolyte.
[e] Two-electron processes.
[f] Averaged value (see text).
[g] R = Me.

148.3(4) and 40.3(5)°, respectively. A different conformation is observed for **6**$(PF_6)_2$. Here, each Bbipy substituent is placed in a position close to the central iron atom of the attached ferrocenyl unit (Fe···COG = 3.801 Å, COG: center of gravity of the B(1)N(21)-C(22)C(32)N(31) ring; O(1)–B(1)–C(11)–C(12) = −99.9(4)°). The two FcBbipy moieties in **6**$(PF_6)_2$ adopt a sterically favorable s-*trans* conformation with respect to the hydroquinone bridge [Fc: $(C_5H_5)Fe(C_5H_4)$].

Both in **4**PF_6 and in **7**PF_6, the cationic moiety is bound to the respective PF_6^- counterion via an OH···F hydrogen bridge.

2.4. Electrochemistry

Paralleling the behavior of **A1** (R = Me) [8], complex **4**PF_6 exhibits both a ferrocene-centered one-electron oxidation and two separate 2,2′-bipyridylboronium-centered one-electron reductions (Table 3). In dichloromethane, as well as in dimethylformamide solutions, the oxidation step possesses features of chemical reversibility in the short time range of cyclic voltammetry as well as during macroelectrolysis. Upon one-electron removal, the original violet solution (λ_{max} = 528 nm) assumes the blue color (λ_{max} = 625 nm) typical of iron-centered ferrocenium species. The reduction processes also display features of chemical reversibility in cyclic voltammetry (Table 3), even though they are affected by electrode adsorption phenomena, which required cleaning of the electrode surface after each cycle. In addition, the second reduction step is accompanied by chemical complications, which are, however, retarded in DMF compared to CH_2Cl_2.

The electrochemical properties of **7**PF_6 are similar to those of **4**PF_6, except for the presence of a further irreversible anodic process attributable to the oxidation of the hydroquinone substituent (Table 3). Again, the reduction processes appear to be accompanied by chemical complications.

Finally, Fig. 5, which shows the cyclic voltammetric behavior of **6**$(PF_6)_2$ in DMF solution, exhibits a coulometrically measured two-electron oxidation, a first two-electron reduction wave displaying features of chemical reversibility and a second irreversible reduction wave (Table 3). The latter is split into two very close maxima. The anodic step can easily be assigned to the concomitant oxidation of the two ferrocenyl units, which are apparently not electronically communicating. Exhaustive two-electron oxidation causes the original violet solution (λ_{max} = 545 nm) to turn blue (λ_{max} = 627 nm). The cathodic pattern indicates a lack of electronic interaction between the two bipyridylboronium units, too, since the first electron addition to the two groups proceedes simultaneously. Only the second electron ad-

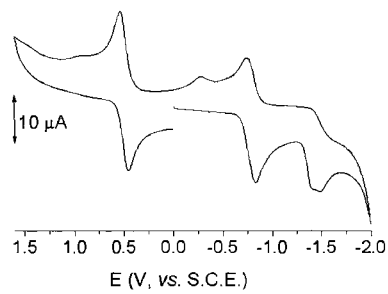

Fig. 5. Cyclic voltammogram recorded at a platinum electrode on a DMF solution containing $[NEt_4](PF_6)$ (0.1 mol dm^{-3}) and **6**$(PF_6)_2$ (0.9×10^{-3} mol dm^{-3}). Scan rate 0.2 V s^{-1}.

dition causes a slight coulombic effect. In contrast to **7**PF_6, no oxidation of the hydroquinone spacer takes place in the solvent window.

3. Conclusions

Complexes **1**Br and **2**Br_2 with one and two $[B(Br)bipy]^+$ substituents covalently attached to a ferrocene core are promising building blocks for the synthesis of larger, highly redox-active aggregates. The reaction of two equivalents of **1**Br with one equivalent of hydroquinone, for example, gives the dinuclear species **6**$(PF_6)_2$, in which the monomeric units are linked via their boron atoms by a [–O–C_6H_4–O–] bridge. According to cyclic voltammetry, **6**$(PF_6)_2$ undergoes three redox transitions resulting in an overall transfer of six electrons. From **2**Br_2 and excess glycol, the 2-hydroxyethoxy substituted complex **5**$(PF_6)_2$ is obtained. Work is in progress to polymerize this compound using well-established polyester or polyurethane chemistry.

4. Experimental

4.1. General considerations

All reactions and manipulations of air-sensitive compounds were carried out in dry, oxygen-free Ar using standard Schlenk ware. Solvents were freshly distilled under N_2 from Na/K alloy-benzophenone (toluene, hexane) or from CaH_2 (CH_2Cl_2, CH_3CN) prior to use. NMR: JEOL JMN-GX 400, Bruker ACP 200, Bruker DPX 250 spectrometer. ^{11}B-NMR spectra are reported relative to external $BF_3{\cdot}Et_2O$. Unless stated otherwise, all NMR spectra were run at ambient temperature; abbreviations: s = singlet; d = doublet; t = triplet; vtr = virtual triplet; m = multiplet; n.r. = multiplet expected in the ^{1}H-NMR spectrum but not resolved; n.o. = signal not observed, bipy = 2,2′-bipyridine, ph = phenylene ring of hydroquinone. Elemental analyses were performed by the microanalytical laboratory of the University of Frankfurt. **1**Br and **2**Br_2 were synthesized according to literature procedures [8].

4.2. Synthesis of **4**PF_6

1Br (0.26 g, 0.51 mmol) was dissolved in glycol (5 ml) at room temperature (r.t.), and neat NEt_3 (0.05 g, 0.50 mmol) was added to the resulting purple solution. The mixture was stirred for 12 h and diluted with 20 ml of H_2O. The clear purple solution was added dropwise into an aqueous solution of NH_4PF_6 (0.17 g, 1.04 mmol), whereupon **4**PF_6 precipitated as a microcrystalline solid. The precipitate was isolated by filtration, triturated with H_2O (3×10 ml) and Et_2O (10 ml) and dried in vacuo. Yield: 0.19 g, 67%. X-ray quality crystals were grown by gas phase diffusion of Et_2O into an actonitrile solution of **4**PF_6 at ambient temperature.

^{11}B-NMR (128.3 MHz, CD_3CN): δ 9.4 ($h_{1/2} = 130$ Hz). ^{1}H-NMR (400.0 MHz, CD_3CN): δ 9.01 (d, 2H, $^3J(HH) = 5.0$ Hz, bipy-6,6′), 8.65 (m, 4H, bipy-3,3′,4,4′), 8.13 (vtr, 2H, $^3J(HH) = 5.0$ Hz, bipy-5,5′), 4.20, 3.89 ($2 \times$ n.r., 2×2H, C_5H_4), 3.92 (s, 5H, C_5H_5), 3.47, 3.13 (t, 2×2H, $^3J(HH) = 4.8$ Hz, –CH_2CH_2–), 2.66 (br, 1H, OH). ^{13}C-NMR (100.6 MHz, CD_3CN): δ 146.7 (bipy-4,4′), 145.6 (bipy-2,2′), 145.1 (bipy-6,6′), 130.0 (bipy-5,5′), 123.9 (bipy-3,3′), n.o. (C_5H_4-*ipso*), 71.9, 70.8 (C_5H_4), 69.3 (C_5H_5), 66.0, 63.5 (–CH_2CH_2–). FABMS: m/z 558 [M^+; 4%], 413 [($M^+ - PF_6$); 100%]. Anal. Found: C, 47.17; H, 4.22; N, 5.00. Calc. for $C_{22}H_{22}BF_6FeN_2O_2P$ (558.05): C, 47.35; H, 3.97; N, 5.02.

4.3. Synthesis of **5**$(PF_6)_2$

5$(PF_6)_2$ was synthesized similar to **4**PF_6 from **2**Br_2 (0.28 g, 0.33 mmol), glycol (5 ml), NEt_3 (0.07 g, 0.67 mmol) and NH_4PF_6 (0.22 g, 1.35 mmol).Yield: 0.20 g, 65%.

^{11}B-NMR (128.3 MHz, CD_3CN): δ 10.4 ($h_{1/2} = 230$ Hz). ^{1}H-NMR (400.0 MHz, CD_3CN): δ 9.04 (d, 4H, $^3J(HH) = 5.0$ Hz, bipy-6,6′), 8.64 (m, 8H, bipy-3,3′,4,4′), 8.13 (vtr, 4H, $^3J(HH) = 5.0$ Hz, bipy-5,5′), 3.97, 3.72 ($2 \times$ n.r., 2×4H, C_5H_4), 3.47, 3.08 (m, t, 2×4H, $^3J(HH) = 4.8$ Hz, –CH_2CH_2–), 2.79 (br, 2H, OH). ^{13}C-NMR (100.6 MHz, CD_3CN): δ 146.8 (bipy-4,4′), 145.5 (bipy-2,2′), 145.2 (bipy-6,6′), 130.0 (bipy-5,5′), 123.9 (bipy-3,3′), n.o. (C_5H_4-*ipso*), 72.0, 71.3 (C_5H_4), 65.7, 63.4 (–CH_2CH_2–). FABMS: m/z 785 [($M^+ - PF_6$); 100%]. Anal. Found: C, 43.67; H, 3.67; N, 5.88. Calc. for $C_{34}H_{34}B_2F_{12}FeN_4O_4P_2$ (930.06): C, 43.91; H, 3.68; N, 6.02.

4.4. Synthesis of **6**$(PF_6)_2$

A slurry of hydroquinone (0.11 g, 0.97 mmol) in 20 ml of CH_2Cl_2 was treated with neat NEt_3 (0.20 g, 1.98 mmol) and cooled to -40 °C. **1**Br (0.99 g, 1.93 mmol) in 40 ml of CH_2Cl_2 was slowly added, the resulting blue mixture was allowed to warm to r.t. and stirred for 12 h. Insoluble material was collected on a frit (G3), dissolved in water (200 ml) and added dropwise to excess NH_4PF_6 (0.65 g, 4.00 mmol) in water (50 ml). The resulting purple precipitate was isolated by filtration, triturated with Et_2O (150 ml) and dried in vacuo. Yield: 1.30 g, 61%. X-ray quality crystals were grown by gas phase diffusion of Et_2O into an actonitrile solution of **6**$(PF_6)_2$ at ambient temperature.

^{11}B-NMR (64.2 MHz, CD_3CN): δ 12.3 ($h_{1/2} = 1625$ Hz). ^{1}H-NMR (250.1 MHz, CD_3CN): δ 9.02 (d, 4H, $^3J(HH) = 5.6$ Hz, bipy-6,6′), 8.62 (vtr, 4H, $^3J(HH) =$

8.0 Hz, bipy-4,4′), 8.50 (d, 4H, $^3J(HH) = 8.0$ Hz, bipy-3,3′), 8.10 (m, 4H, bipy-5,5′), 6.03 (s, 4H, ph), 4.25, 3.95 ($2 \times$ n.r., 2×4H, C_5H_4), 3.99 (s, 10H, C_5H_5). ^{13}C-NMR (62.9 MHz, CD_3CN): δ 150.9 (ph-*ipso*), 146.9 (bipy-4,4′), 145.0 (bipy-2,2′), 144.9 (bipy-6,6′), 130.0 (bipy-5,5′), 123.6 (bipy-3,3′), 122.0 (ph-*C*H), n.o. (C_5H_4-*ipso*), 71.7, 70.9 (C_5H_4), 69.1 (C_5H_5). FABMS of **6**$(PF_6)_2$: m/z 1102 [M^+; 2%], 957 [($M^+ - PF_6$); 20%], 812 [($M^+ - 2PF_6$); 7%]. Anal. Found: C, 50.33; H, 3.68; N, 5.08. Calc. for $C_{46}H_{38}B_2F_{12}Fe_2N_4O_2P_2$ (1102.07): C, 50.13; H, 3.48; N, 5.08.

4.5. Synthesis of 7Br and 7PF_6

A CH_2Cl_2 (60 ml) solution of **1**Br (0.13 g, 0.26 mmol) was added dropwise with stirring at r.t. to hydroquinone (0.03 g, 0.27 mmol) and NEt_3 (0.03 g, 0.30 mmol) in 10 ml of CH_2Cl_2. The resulting mixture was stirred overnight, whereupon a purple microcrystalline solid slowly precipitated. Insoluble material was collected on a frit, triturated with Et_2O (2×20 ml) and dried in vacuo. Yield: 0.10 g, 71%.

^{11}B-NMR (64.2 MHz, Me_2SO-d_6): δ -3.7 ($h_{1/2} =$ 772 Hz). ^{1}H-NMR (250.1 MHz, Me_2SO-d_6): δ 9.45 (d, 2H, $^3J(HH) = 5.4$ Hz, bipy-6,6′), 8.98 (d, 2H, $^3J(HH) = 8.0$ Hz, bipy-3,3′), 8.87 (s, 1H, OH), 8.81 (vtr, 2H, $^3J(HH) = 8.0$ Hz, bipy-4,4′), 8.32 (vtr, 2H, $^3J(HH) = 6.6$ Hz, bipy-5,5′), 6.34 (d, 2H, $^3J(HH) =$ 9.0 Hz, ph-2,6), 6.26 (d, 2H, $^3J(HH) = 9.0$ Hz, ph-3,5), 4.27, 4.11 ($2 \times$ n.r., 2×2H, C_5H_4), 3.99 (s, 5H, C_5H_5). ^{13}C-NMR (62.9 MHz, Me_2SO-d_6): δ 152.1 (ph-4), 147.3 (ph-1), 146.4 (bipy-4,4′), 144.6 (bipy-2,2′), 144.0 (bipy-6,6′), 129.3 (bipy-5,5′), 123.2 (bipy-3,3′), 120.9 (ph-2,6), 115.6 (ph-3,5), n.o. (C_5H_4-*ipso*), 71.1, 69.7, (C_5H_4), 68.2 (C_5H_5). Anal. Calcd. for $C_{26}H_{22}BBrFeN_2O_2$ (541.03) $\times$ H_2O (18.02): C, 55.86; H, 4.33; N, 5.01. Found: C, 55.50; H, 4.35; N, 5.10.

7Br (0.07 g, 0.13 mmol) was dissolved in 20 ml of H_2O and added to an aqueous solution of NH_4PF_6 (0.04 g, 0.25 mmol), whereupon **7**PF_6 precipitated. The precipitate was isolated by filtration, triturated with H_2O (2×10 ml) and Et_2O (10 ml) and dried in vacuo. X-ray quality crystals were grown by gas phase diffusion of Et_2O into an actonitrile solution of **7**PF_6 at ambient temperature.

4.6. Crystal data of 4PF_6

A black needle of **4**PF_6 was mounted on top of a glass filament on a CCD Diffraction System (Bruker AXS). Final lattice parameters were obtained by least-squares refinement of 7864 reflections. Data were collected with a crystal-to-detector distance of 50 mm ($1.8° < \theta < 26.02°$). Data were corrected for Lorentz and polarization terms; an empirical absorption correction was applied [13]. The structure was solved by direct methods [14] and refined against F^2 with full-matrix least-squares methods [15]. Hydrogen atoms bonded to C were calculated in ideal positions (riding model). The hydroxyl-H atom was refined freely. A total of 320 parameters refined, 13.9 data per parameter, $w = 1/[\sigma^2(F_o^2) + (0.0473P)^2 + 1.8562P]$ where $P = (F_o^2 + 2F_c^2)/3$, shift/error < 0.001 in the last cycle of refinement, residual electron density $+0.613$ e Å^{-3}/ -0.387 e Å^{-3}, $R_1 = 0.0418$, $wR_2 = 0.0937$ [$I > 2\sigma(I)$], minimized function was $\Sigma w((F_o^2) - (F_c^2))^2$.

4.7. Crystal data of 6$(PF_6)_2$

A red needle of **6**$(PF_6)_2$ was mounted on top of a glass filament on a CCD Diffraction System (Bruker AXS). Final lattice parameters were obtained by least-squares refinement of 510 reflections. Data were collected with a crystal-to-detector distance of 40 mm ($1.78° < \theta < 28.70°$). Data were corrected for Lorentz and polarization terms; an empirical absorption correction was applied [13]. The structure was solved by direct methods [14] and refined against F^2 with full-matrix least-squares methods [15]. Hydrogen atoms were calculated in ideal positions (riding model). A total of 344 parameters refined, 18.3 data per parameter, $w = 1/[\sigma^2(F_o^2) + (0.0382P)^2 + 0.991P]$ where $P = (F_o^2 + 2F_c^2)/3$, shift/error < 0.001 in the last cycle of refinement, residual electron density $+0.425$ e Å^{-3}, -0.431 e Å^{-3}, $R_1 = 0.0601$, $wR_2 = 0.0905$ [$I > 2\sigma(I)$], minimized function was $\Sigma w((F_o^2) - (F_c^2))^2$.

4.8. Crystal data of 7PF_6

A brown–black needle of **7**$PF_6 \cdot 0.5C_4H_{10}O$ was mounted on top of a glass filament on a CCD Diffraction System (Bruker AXS). Final lattice parameters were obtained by least-squares refinement of 5419 reflections. Data were collected with a crystal-to-detector distance of 40 mm ($1.79° < \theta < 25.68°$). Data were corrected for Lorentz and polarization terms; an empirical absorption correction was applied [13]. The structure was solved by direct methods [14] and refined against F^2 with full-matrix least-squares methods [15]. Hydrogen atoms bonded to C were calculated in ideal positions (riding model). The hydroxyl-H atom was refined freely. A total of 376 parameters refined, 14.2 data per parameter, $w = 1/[\sigma^2(F_o^2) + (0.0570P)^2 + 0.6507P]$ where $P = (F_o^2 + 2F_c^2)/3$, shift/error < 0.024 in the last cycle of refinement, residual electron density $+0.720$ e Å^{-3}, -0.442 e Å^{-3}, $R_1 = 0.0526$, $wR_2 = 0.1094$ [$I > 2\sigma(I)$], minimized function was $\Sigma w((F_o^2) - (F_c^2))^2$.

Acknowledgements

This work was supported by the 'Deutsche Forschungsgemeinschaft' and the 'Fonds der Chemischen Industrie'. L.D. is grateful to the Alexander von Humboldt foundation for a postdoc grant. P.Z. acknowledges financial funding by the University of Siena (PAR 1999).

References

[1] O. Kahn, Acc. Chem. Res. 33 (2000) 647.
[2] P. Nguyen, P. Gómez-Elipe, I. Manners, Chem. Rev. 99 (1999) 1515.
[3] I. Cuadrado, M. Morán, C.M. Casado, B. Alonso, J. Losada, Coord. Chem. Rev. 193–195 (1999) 395.
[4] B. Jiang, S.W. Yang, S.L. Bailey, L.G. Hermans, R.A. Niver, M.A. Bolcar, W.E. Jones Jr., Coord. Chem. Rev. 171 (1998) 365.
[5] R.J. Mortimer, Chem. Soc. Rev. 26 (1997) 147.
[6] C.U. Pittman Jr., C.E. Carraher Jr., M. Zeldin, J.E. Sheats, B.M. Culbertson (Eds.), Metal-Containing Polymeric Materials, Plenum Press, New York, 1996.
[7] O. Kahn, Molecular Magnetism, Wiley–VCH, New York, 1993.
[8] F. Fabrizi de Biani, T. Gmeinwieser, E. Herdtweck, F. Jäkle, F. Laschi, M. Wagner, P. Zanello, Organometallics 16 (1997) 4776.
[9] S. Hünig, I. Wehner, Heterocycles 28 (1989) 359.
[10] L. Ding, K. Ma, F. Fabrizi de Biani, M. Bolte, P. Zanello, M. Wagner, Organometallics 20 (2001) 1041.
[11] K. Ma, M. Wagner, unpublished results.
[12] H. Nöth, B. Wrackmeyer, Nuclear Magnetic Resonance Spectroscopy of Boron Compounds, Springer, Berlin, 1978.
[13] G.M. Sheldrick, SADABS: A Program for Empirical Absorption Correction of Area Detector Data, Universität Göttingen, Germany, 1996.
[14] G.M. Sheldrick, Acta Crystallogr. A46 (1990) 467.
[15] G.M. Sheldrick, SHELXL-97. A Program for the Refinement of Crystal Structures, Universität Göttingen, Germany, 1997.